Известия Саратовского университета. Новая серия. Серия: Физика. 2024. Т. 24, вып. 2. С. 161–170
Izvestiya of Saratov University. Physics, 2024, vol. 24, iss. 2, pp. 161–170
https://fizika.sgu.ru https://doi.org/10.18500/1817-3020-2024-24-2-161-170, EDN: MYMUHS

Article

Kinetics of glycerol-induced molecular diffusion in the normal and cancerous ovarian tissues

A. A. Selifonov[1,2✉], **A. M. Zakharevich**[1], **A. S. Rykhlov**[3], **V. V. Tuchin**[1,4,5]

[1]Saratov State University, 83 Astrakhanskaya St., Saratov 410012, Russia
[2]Saratov State Medical University named after V. I. Razumovsky, 112 Bol'shaya Kazach'ya St., Saratov 410012, Russia
[3]Saratov State University of Genetics, Biotechnology and Engineering named after N. I. Vavilov, Clinic "Veterinary Hospital", 220 Bol'shaya Sadovaya St., Saratov 410012, Russia
[4]Tomsk State University, 36 Lenina Ave., Tomsk 634050, Russia
[5]Institute of Precision Mechanics and Control, FRS "Saratov Scientific Centre of the RAS", 24 B Rabochaya St., Saratov 410028, Russia

Alexey A. Selifonov, peshka029@gmail.com, https://orcid.org/0000-0002-6270-9395
Andrey M. Zakharevich, lab-15@mail.ru, https://orcid.org/0000-0002-3813-5870
Andrey S. Rykhlov, rychlov.andrej@yandex.com, https://orcid.org/0000-0003-1194-9548
Valery V. Tuchin, tuchinvv@mail.ru, https://orcid.org/0000-0001-7479-2694

Abstract. ***Background and Objectives***. There is a global trend towards an increase in the number of patients diagnosed with ovarian cancer during their reproductive years. One of the current clinical technologies is the technology of cryopreservation of removed healthy ovaries in order to preserve fertility and their subsequent transplantation after treatment for cancer of other organs. Glycerol is often used as a non-penetrating agent in freezing to improve follicle survival. ***Materials and Methods*****.** The work examined the ovaries of cats with diagnoses confirmed by histological studies: follicular phase, luteal phase, serous carcinoma, leimyosarcoma. Diffuse reflectance spectroscopy was used to determine the kinetic parameters of dehydration and optical properties of tissues upon interaction with glycerol. Based on the change in mass over a long period of time, the diffusion coefficient of glycerol in the samples was determined. ***Results*****.** The effective diffusion coefficient of interstitial water in cat ovarian tissue has been measured: $D = (2.6 \pm 0.4)\cdot 10^{-6}$ cm^2/s (follicular phase), $D = (3.3 \pm 0.4)\cdot 10^{-6}$ cm^2/s (luteal phase), $D = (3.0 \pm 0.3)\cdot 10^{-6}$ cm^2/s (leiomyosarcoma), and $D = (1.6 \pm 0.2)\cdot 10^{-6}$ cm^2/s (serous carcinoma), which is initiated within 1.5–2 hours of interaction. Diffusion of glycerol occurs over a long period of time, about 400 hours, and for the samples under study is: $D = (8.3 \pm 2.5)\cdot 10^{-8}$ cm^2/s (follicular phase), $D = (5.6 \pm 1.7)\cdot 10^{-8}$ cm^2/s (luteal phase), $D = (2.2 \pm 0.2)\cdot 10^{-8}$ cm^2/s (leiomyosarcoma), and $D = (1.1 \pm 0.4)\cdot 10^{-7}$ cm^2/s (serous carcinoma). ***Conclusion*****.** The established perfusion-kinetic parameters of glycerol/interstitial water for the studied samples can be used in clinical practice in the preparation of ovarian tissue for transplantation (cryopreservation), in the transmembrane transfer of drugs, the development of new reproductive technologies, etc.

Keywords: ovarian tissues, follicular phase, luteal phase, serous carcinoma, leimyosarcoma, glycerol, interstitial water, diffuse reflectance spectra, diffusion coefficient

Acknowledgements: The study was supported by the Russian Science Foundation (project No. 22-75-00021).

For citation: Selifonov A. A., Zakharevich A. M., Rykhlov A. S., Tuchin V. V. Kinetics of glycerol-induced molecular diffusion in the normal and cancerous ovarian tissues. *Izvestiya of Saratov University. Physics*, 2024, vol. 24, iss. 2, pp. 161–170. https://doi.org/10.18500/1817-3020-2024-24-2-161-170, EDN: MYMUHS

Научная статья
УДК 535.341.08:535.346.1

Кинетика индуцированной глицерином молекулярной диффузии в нормальных и раковых тканях яичников

А. А. Селифонов [1,2✉], **А. М. Захаревич**[1], **А. С. Рыхлов**[3], **В. В. Тучин**[1,4,5]

[1]Саратовский национальный исследовательский государственный университет имени Н. Г. Чернышевского, Россия, 410012, Саратов, ул. Астраханская, д. 83
[2]Саратовский государственный медицинский университет им. В. И. Разумовского Минздрава России, Россия, 410012, г. Саратов, ул. Большая Казачья, д. 112
[3]Саратовский государственный университет генетики, биотехнологии и инженерии им. Н. И. Вавилова, Ветеринарный Госпиталь, Россия, 410012, г. Саратов, ул. Большая Садовая, д. 220
[4]Национальный исследовательский Томский государственный университет, Лаборатория лазерной молекулярной визуализации и машинного обучения, Россия, 634050, г. Томск, пр. Ленина, д. 36
[5]Институт проблем точной механики и управления, Саратовский научный центр РАН, Россия, 410028, г. Саратов, ул. Рабочая, д. 24 Б

Селифонов Алексей Андреевич, peshka029@gmail.com, https://orcid.org/0000-0002-6270-9395
Захаревич Андрей Михайлович, lab-15@mail.ru, https://orcid.org/0000-0002-3813-5870
Рыхлов Андрей Сергеевич, rychlov.andrej@yandex.ru, https://orcid.org/0000-0003-1194-9548
Тучин Валерий Викторович, tuchinvv@mail.ru, https://orcid.org/0000-0001-7479-2694

Аннотация. ***Предыстория и цели***. Существует глобальная тенденция к увеличению числа пациентов с диагнозом рак яичников в течение их репродуктивного возраста. Одной из нынешних клинических технологий является технология криоконсервации удаленных здоровых яичников, чтобы сохранить фертильность и их последующую трансплантацию после лечения рака других органов. Глицерин часто используется в качестве непроникающего агента при замораживании органов для улучшения выживаемости фолликулов. ***Материалы и методы***. В работе изучались яичники кошек с диагнозами, подтвержденными гистологическими исследованиями: фолликулярная фаза, лютеиновая фаза, серозная карцинома, леймиосаркома. Диффузная спектроскопия отражения использовалась для определения кинетических параметров дегидратации и оптических свойств тканей при взаимодействии с глицерином. По изменению массы в течение длительного времени определяли коэффициент диффузии глицерина в образцах. ***Полученные результаты***. Был измерен эффективный коэффициент диффузии интерстициальной воды для яичников кошек: $D = (2.6 \pm 0.4)\cdot 10^{-6}$ см^2/с (фолликулярная фаза), $D = (3.3 \pm 0.4)\cdot 10^{-6}$ см^2/с (лютеиновая фаза), $D = (3.0 \pm 0.3)\cdot 10^{-6}$ см^2/с (лейомиосаркома), $D = (1.6 \pm 0.2)\cdot 10^{-6}$ см^2/с (серозная карцинома), который инициируется через 1.5–2 часа после взаимодействия образцов с глицерином. Диффузия глицерина происходит в течение длительного периода времени, около 400 часов, и для исследуемых образцов составляет: $D = (8.3 \pm 2.5)\cdot 10^{-8}$ см^2/с (фолликулярная фаза), $D = (5.6 \pm 1.7)\cdot 10^{-8}$ см^2/с (лютеиновая фаза), $D = (2.2 \pm 0.2)\cdot 10^{-8}$ см^2/с (леймиосаркома) и $D = (1.1 \pm 0.4)\cdot 10^{-7}$ см^2/с (серозная карцинома). ***Выводы***. Установленные перфузионно-кинетические свойства глицерина/интерстициальной воды для изучаемых образцов могут использоваться в клинической практике при приготовлении ткани яичников для трансплантации (криоконсервации), при трансмембранном переносе лекарств, развитии новых репродуктивных технологий и т. д.

Ключевые слова: ткани яичников, фолликулярная фаза, лютеиновая фаза, серозная карцинома, леймиосаркома, глицерин, интерстициальная вода, спектры диффузного отражения, коэффициент диффузии

Благодарности: Работа выполнена при финансовой поддержке Российского научного фонда (проект № 22-75-00021).

Для цитирования: Selifonov A. A., Zakharevich A. M., Rykhlov A. S., Tuchin V. V. Kinetics of glycerol-induced molecular diffusion in the normal and cancerous ovarian tissues [*Селифонов А. А., Захаревич А. М., Рыхлов А. С., Тучин В. В.* Кинетика индуцированной глицерином молекулярной диффузии в нормальных и раковых тканях яичников] // Известия Саратовского университета. Новая серия. Серия: Физика. 2024. Т. 24, вып. 2. С. 161–170. https://doi.org/10.18500/1817-3020-2024-24-2-161-170, EDN: MYMUHS

1. Introduction

Among all oncogynecological pathologies, mortality from ovarian cancer is in first place in terms of mortality, and in almost half of the cases (47%) mortality from genital cancer is caused by ovarian cancer. Despite a significant amount of both theoretical and clinical research, the causes of most ovarian tumors remain unknown. The largest role in the development of ovarian cancer is currently assigned to hormonal and genetic factors [1]. One of the main methods for diagnosing the female reproductive system is ultrasound, as a fairly informative, simple, fast, harmless, painless method. The most informative method is laparoscopy. During laparoscopy, a video camera is used to examine the pelvic organs, which are formed mainly due to the reflection of light, since there is a strong scattering of light [2]. By using optical immersion clearing, it is possible to reversibly reduce strong tissue scattering and reveal hidden pathologies within the organ [3–5]. The next stage of in-depth diagnosis of ovarian cancer may be X-ray computed tomography (CT) or magnetic resonance imaging (MRI) in cases where echography does not provide a clear idea of the extent of tumor damage. Glycerol, CT and MRI contrast agents are good optical clearing agents [6, 7], therefore a combination of endoscopic or laparoscopic optical, CT and MRI examination with high-resolution and enhanced contrast can be provided.

Optical diagnostic methods, in particular optical coherence tomography, are effectively used [8]. When testing the first laparoscopic OCT probe, it is possible to study the preliminary features of the microstructure of normal ovaries, endometriosis, as well as benign and malignant neoplasms of the surface epithelium of human ovaries [9]. Full-field optical coherence tomography was used to classify normal and malignant human ovarian tissue [10].

An automated platform is proposed that learns to detect ovarian cancer in transgenic mice from optical coherence tomography recordings using a neural network [11]. The endoscopic system used in laparoscopic interventions, which included integrated optical coherence tomography, ultrasound, and photoacoustic imaging, is superior to characterizing ovarian tissue than either method alone [12]. Currently, there is an increase in the number of cancer diseases among patients of reproductive age [13]. When a tumor process is detected, patients are prescribed complex chemotherapy and radiation therapy, which most likely leads to complete or

partial loss of fertility [14]. In a group of young patients with cancer, impaired reproductive function or premature ovarian failure, it is possible to preserve reproductive function using cryopreservation. Freezing (cryopreservation) of healthy ovarian tissue is a relatively new clinical method for organ transplantation after recovery [15]. Often cryopreservation of ovarian tissue is carried out by freezing using cryoprotectants: dimethyl sulfoxide (DMSO), ethylene glycol and 1,2-propanediol [4]. Slow freezing has a significant drawback – the risk of cell damage from ice crystals [16].

The use of glycerol in cryopreservation of ovarian tissue can be useful for maintaining the viability of follicles, since glycerol causes cell dehydration and, when mixed with water, reduces the temperature of ice formation in cells and solutions and increases the viscosity of aqueous solutions.

In this work, we studied the permeability of the healthy cat ovaries in different phases of the cycle (follicular and luteal) and ovaries with cancer lesions (serous carcinoma and leimyosarcoma) induced by glycerol application. Based on the optically measured kinetics of glycerol/interstitial water perfusion for thick tissue sections, quantified by the effective molecular diffusion coefficient, the dehydration time of the entire organ was determined. The efficiency and time of optical clearing of the studied samples, as well as histological changes and tissue microstructure in normal conditions and in pathologies, were also determined.

2. Materials and Methods

The samples for research in this work were the ovaries of outbred cats aged 3 to 10 years, obtained after ovariectomy and ovariohysterectomy in a veterinary hospital. For histological examination of all samples, hematoxylin-eosin staining was used. Chemically pure glycerol 99.5% (Akrichimpharm LLC, Russia) was used as an optical clearing agent. The following ovaries were studied: 1 – healthy in the follicular phase; 2 – healthy in the luteal phase; 3 – with a diagnosis of leimyosarcoma and 4 – serous ovarian cancer. The diagnosis of all studied samples was specified in the histological report.

The thickness of tissue sections (samples placed between glass slides) was measured with an electron micrometer (Union Source CO., Ltd., China, Ningbo) at several points on the sample and then averaged. The accuracy of each measurement was ± 0.01 mm. The average thickness of ovarian sections was (0.90 ± 0.09) mm.

To measure the diffuse reflectance spectra (DRS) of tissue samples in the spectral range of 200–800 nm, a Shimadzu UV-2550 dual-beam spectrophotometer (Japan) with an integrating sphere was used (Fig. 1). The radiation source was a halogen lamp with radiation filtering in the spectral range under study. The maximum resolution of the spectrometer was 0.1 nm. Before measurements, the spectra were normalized using a $BaSO_4$ reference reflector. All measurements were carried out at room temperature ($\sim$25°C) and normal atmospheric pressure.

Determination of the glycerol/interstitial water diffusion coefficient in tissues is based on measurements of DRS kinetics, use of the free diffusion model and Fick's second law and modified Bouguer – Beer – Lambert law. The experimental conditions and calculation methods are described in more detail in [17]. In brief, expression for the dif-

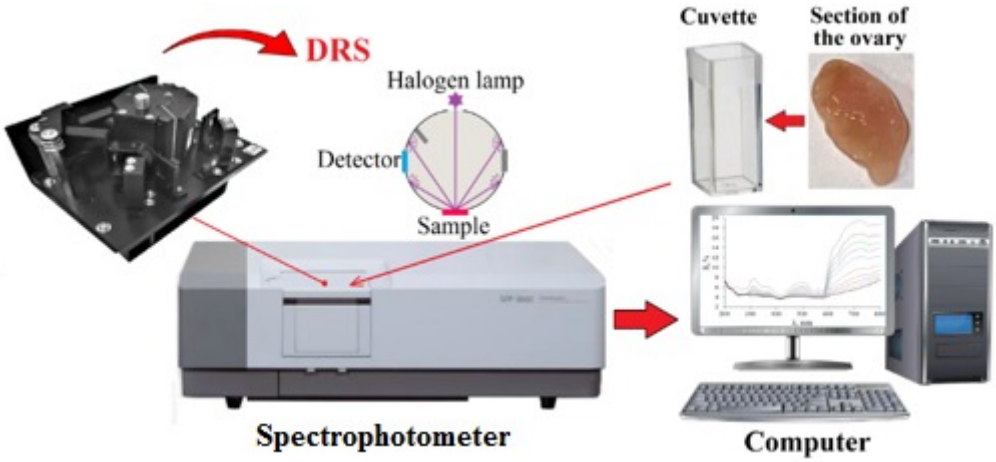

Figure. 1. Scheme of the experimental setup for measuring DRS of cat ovarian tissue samples (color online)

ference between the effective optical density at the current time $A(t, \lambda)$ and at the initial time $A(t = 0, \lambda)$

$$\Delta A(t,\lambda) = A(t,\lambda) - A(t=0,\lambda) \sim C_0\{1 - \exp(t/\tau)\}, \quad (1)$$

where the effective optical density is determined from the measurements of DRS (R_d)

$$A = -\log R_d; \quad (2)$$

t is the time during which the diffusion process occurs, s; λ is the wavelength in nm;

C_0 is the initial concentration of the glycerol, mol/l; τ is the effective diffusion time, s,

$$\tau = 4l^2/\pi^2 D; \quad (3)$$

l is the thickness of the sample under study, mm; D is the effective diffusion coefficient of the glycerol/interstitial water molecules, cm^2/s.

To determine the degree of dehydration, the weight of the samples was measured when they were dried in air and when interacting with glycerol. The samples were weighed using an analytical balance. When air drying, the samples were placed in an oven and dried by heating to a temperature of 39°C. To study the dehydration of samples when interacting with glycerol, the samples were placed in a container with a tight-fitting lid; the volume of glycerol corresponded to the volume of the quartz cuvette when measuring the optical properties of the samples and was 3 ml. Weight measurements were carried out while carefully removing glycerol from the surface of the sample.

The degree of tissue dehydration H_d was calculated, using the following equation, accounting for that sample weight is equal to its mass [18, 19]

$$H_d = \{[M(t=0) - M(t)]/M(t=0)\}, \quad (4)$$

where $M(t = 0)$ and M (t) are the initial and current mass of the sample, respectively, g; t is the time during which the diffusion occurs, s.

The temporal dependence of tissue dehydration can be presented in the following form [18, 19]

$$H_d = A_d \cdot [1 - \exp(-t/\tau)], \quad (5)$$

where A_d is the empirical coefficient; τ is the characteristic dehydration time, which in the case of osmotic action of glycerol is described by equation (3) for diffusion coefficient of water D_w.

The recorded DRS (R_d (λ), %) were converted using the standard Kubelka–Munk algorithm to $A(\lambda)$ extinction spectra (Shimadzu UV-2550 spectrophotometer software). To record the final spectra of diffuse reflectance after the completion of glycerol immersion, tissue samples were placed in clean quartz cuvettes and the spectra were recorded without glycerol.

The protocol of the Local Ethics Committee on permission to conduct these studies (No. 4 dated November 01, 2022) was issued by Saratov State Medical University named after V. I. Razumovsky.

3. Results and Discussion

Ovary in the follicular phase (Fig. 2, a).

Ovary: ovary with preserved histological structure. The cortex is well developed, the ratio area of stroma to parenchyma is approximately 1 : 1.5, the theca tissue is of a typical appearance. Multiple follicles at different stages of maturation are visualized (highlighted with a black frame, Fig. 2, *a*). Atypia, necrosis, invasive growth, mitotic activity, inflammation, colonies of bacteria and fungi are not detected.

Conclusion: the histological picture corresponds to the ovary in the follicular growth phase.

Ovary in the luteal phase (Fig. 2, b).

Corpus luteum with signs of severe hyperplasia without atypia. Ovary: ovary with preserved histological structure. The cortex is moderately developed, the ratio area of stroma to parenchyma is approximately 1 : 2. There is a corpus luteum without atypia and hyperplasia (highlighted with a black frame, Fig. 2, *b*). The stroma is represented by typical theca tissue without edema, is moderately developed, and has thick- and thin-walled vessels.

Conclusion: the histological picture corresponds to the ovary in the luteal phase of growth.

Ovary with leimyosarcoma (Fig. 2, c).

Severe atypical changes with tumor autolytic fragments were revealed. Tumor spindle-shaped atypical cells with a high nuclear-cytoplasmic ratio, with 1-2 eosinophilic nucleoli visible at 400 magnification and fields of tumor necrosis with cell shadows are identified. The degree of nuclear atypia is high, tumor cells form solid fields. The stroma is rather poorly developed, and scant vascularization is visualized. Lymphovascular invasion in the volume of the studied material is not determined. Mitotic activity – 20 mitoses per 10 fields of view at a magnification of 400 (2.5 mm^2).

Conclusion: the morphological picture is most consistent with leiomyosarcoma

Ovary with serous carcinoma (Fig. 2, d).

Theca tissue is represented by spindle-shaped cells with hyperchromic streak-shaped nuclei, indistinguishable intercellular boundaries, and weakly

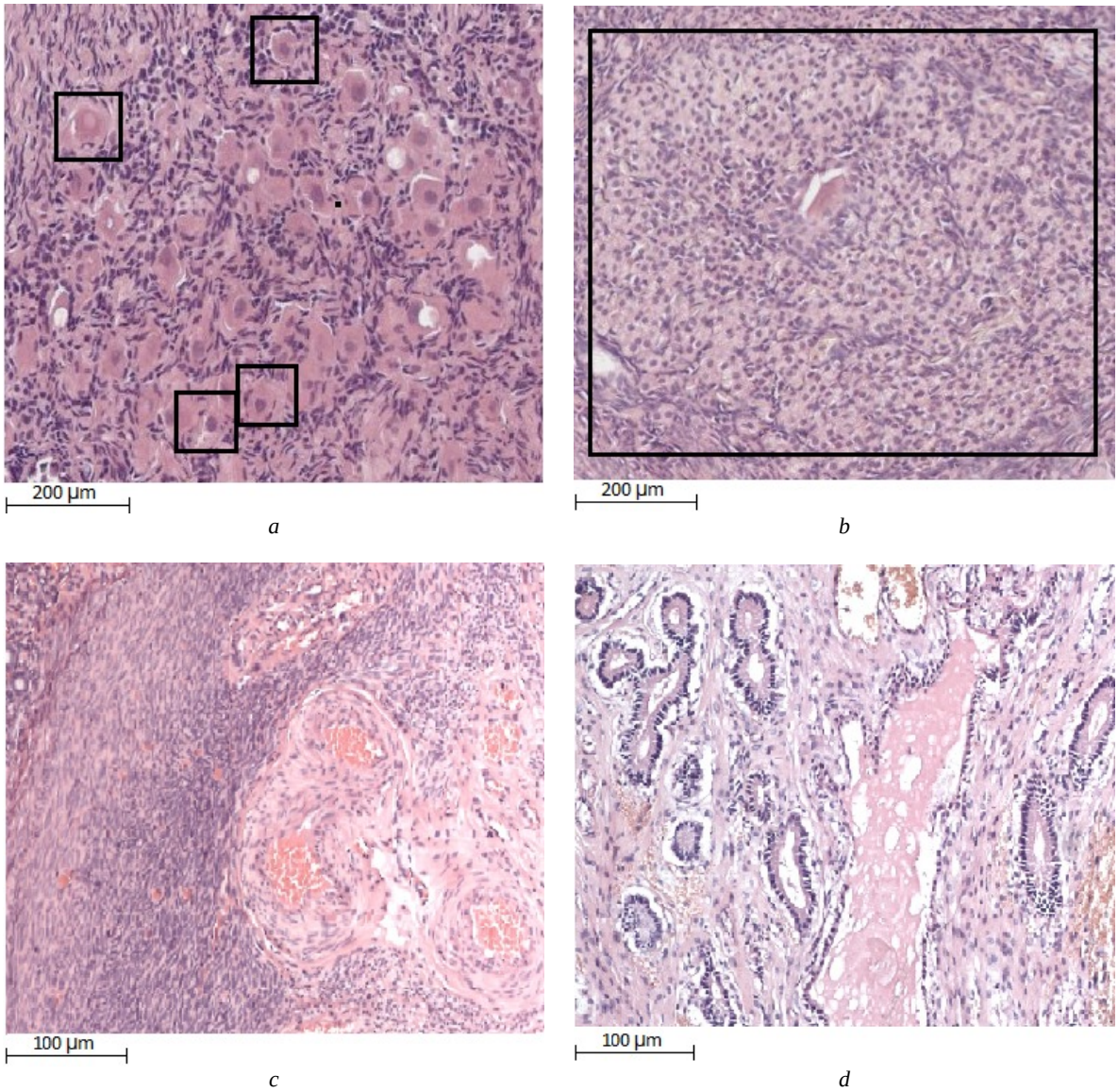

Figure 2. Images of histological sections of cat ovaries in healthy follicular (*a*) and luteal (*b*) phases, and cancerous states with leiomyosarcoma (*c*) and serous carcinoma (*d*) (color online)

eosinophilic cytoplasm. Numerous cystic formations, subepithelial formations are visualized, lined with mononuclear columnar epithelium, flattened in places, with a moderate amount of weakly eosinophilic cytoplasm and monomorphic round hyperchromic nuclei. Large-focal numerous hemorrhages and foci of infiltration by siderophages are identified. In the ovarian tissue, tumor growth is observed, consisting of large, hyperchromatic cells with a small basophilic nucleus and large eosinophilic cytoplasm. Tumor cells form tubular, pseudotubular and solid structures. Mitotic activity – 14 mitoses per 10 fields of view at a magnification of 40. Necrosis is not detected.

Conclusion: The histological picture is consistent with serous ovarian carcinoma.

The optical properties of tissues are responsible for the propagation of radiation inside and outside the studied samples, as well as for its attenuation. In the UV region, the main endogenous chromophores of the studied samples are amino acid residues of proteins (220, 285 nm), collagen (340 nm) and elastin (355 nm), and in the visible region the main chromophore is oxyhemoglobin, which has characteristic bands at 415 (Soret band), 542 and 576 nm (Q-bands), tissue porphyrins (410 nm) and carotenoids (420–490 nm).

Figure 3 shows the average values of diffuse reflectance ($n = 5$) at the initial moment and after

completion of optical clearing of the studied samples. It can be seen that the drops in DRS characteristic of endogenous chromophores are significantly smoothed out in the range from 200 to 800 nm.

Using equations (1) – (3), we found the diffusion time, which in the follicular phase of the ovary of a healthy cat was 21.2 ± 0.8 minutes; 16.3 ± 0.6 min in the luteal phase, 18.3 ± 0.6 min in the ovary with leimyosarcoma; and 35.3 ± 1.8 minutes in the ovary with serous cancer.

This parameter was obtained after approximating experimental data – changes in optical density.

Quantitative perfusion parameters of cat ovaries samples (0.9 mm thick) under the influence of glycerol were obtained using equations (1) – (3): healthy cat ovaries at the follicular phase $D = (2.6 \pm 0.4) \times \times 10^{-6}$ cm^2/s; healthy cat ovaries at the luteal phase $D = (3.3 \pm 0.4) \cdot 10^{-6}$ cm^2/s, ovary with leimyosarcoma $D = (3.0 \pm 0.3) \cdot 10^{-6}$ cm^2/s; and ovary with serous carcinoma $D = (1.6 \pm 0.2) \cdot 10^{-6}$ cm^2/s.

Previously obtained water diffusion coefficients in tissues: $D = (1.9 \pm 0.2) \cdot 10^{-6}$ cm^2/s for the ovaries in the follicular stage of the cycle and $D = (2.4 \pm \pm 0.2) \cdot 10^{-6}$ cm^2/s for the ovaries in the luteal phase of the cycle [20]. The molecular diffusion coefficient measured in human gum tissue under the influence of highly concentrated glycerol (99.5%) was $(1.78 \pm \pm 0.22) \cdot 10^{-6}$ cm^2/s ($n = 5$; $l = 0.59 \pm 0.06$ mm) [21].

The data obtained correlate well with literature data for other tissues, taking into account the structural features of the tissues under study, and are associated primarily with the diffusion of water in tissues due to osmotic stress [22, 23].

In Ref. [24], the effective diffusion coefficients of glycerol/interstitial water in pig ovarian cortex tissue at action of 48%-glycerol aqueous solution were determined: by osmometry $D = (5.99 \pm 2.24) \times \times 10^{-6}$ cm^2/s, by differential scanning calorimetry $D = (5.36 \pm 0.89) \cdot 10^{-6}$ cm^2/s, by infrared spectroscopy with Fourier transform $D = (5.73 \pm 0.81) \times \times 10^{-6}$ cm^2/s. The diffusion coefficients of glycerol (2 M, 4 M and 8 M: which corresponds to 2M $\approx$ 19%, 4M $\approx$ 35%, 8M $\approx$ 65% (at 20 Celsius degree) respectively) in horse ovarian tissue studied by osmometry were: $D = (7.6 \pm 2.9) \cdot 10^{-6}$ cm^2/s, $D = (3.8 \pm 0.8) \times \times 10^{-6}$ cm^2/s, $D = (3.2 \pm 0.8) \cdot 10^{-6}$ cm^2/s [25]. The values we obtained for the effective diffusion coefficients of glycerol/interstitial water in cat ovarian tissue are in good agreement with the values given above and obtained by an independent method, taking into account the high concentration of glycerol used.

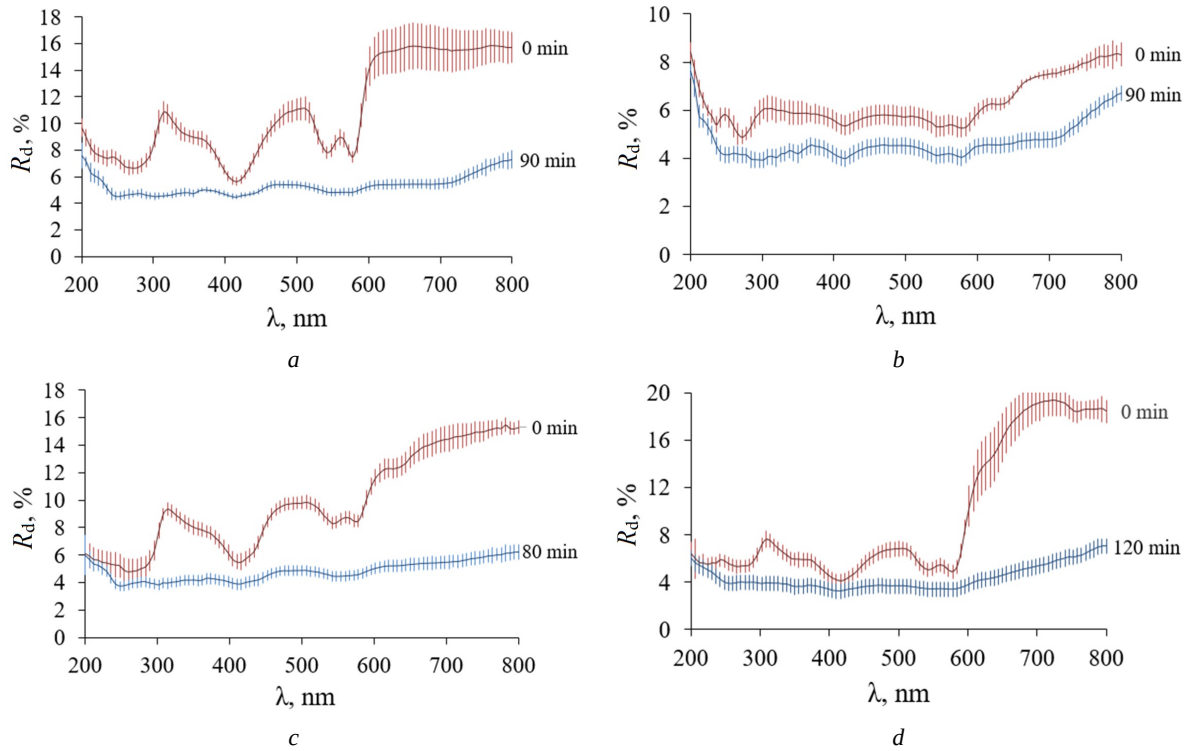

Figure 3. DRS of cat ovary tissue before and after immersion in 99.5% glycerol in the range from 200 to 800 nm: healthy cat ovaries at the follicular phase (*a*); healthy cat ovaries at the luteal phase (*b*), ovary with leimyosarcoma (*c*); ovary with serous carcinoma (*d*) (color online)

Tissue dehydration was studied by measuring the mass of the samples in air and in tightly closed cells during interaction with glycerol (Fig. 4).

The parameters of cat ovarian samples measured and calculated using formulas (4) and (5) are presented in Table.

Thus, the process of interaction of glycerol with samples is associated with dehydration (the influx of interstitial water of biological tissue to the space occupied by the agent and the penetration of glycerol into the sample). The percentage of the mass of interstitial water leaving the sample during evaporation in air relative to the initial mass of the samples was determined: for the ovaries in the luteal phase – 71.1%; in the follicular phase – 72.1%; with leimyosarcoma – 47.9%; and with serous cancer – 76.8%. It has been found that during prolonged interaction with glycerol, after tissue dehydration (low sample mass) glycerol diffuses into the sample (increase of sample mass), this corresponds to the literature data [18].

The change in the mass of the studied samples upon interaction with glycerol over 400 hours is presented in Fig. 5.

The penetration of glycerol into the samples occurs much slower than the extraction of intercellular water from the samples, which in our experiment is 90 ± 30 min (when no change in the DRS and mass of the samples is observed within 30 min). Mass measurements were carried out under the same normal conditions, when stored in 3 ml of glycerol in tightly closed cells. Using the tangent of the slope of the approximation line, the diffusion coefficients of glycerol into the samples were determined. Diffusion of glycerol occurs over a long period of time, about 400 hours, and for the samples under study is characterized by the following diffusion coefficients: $D = (8.3 \pm 2.5) \cdot 10^{-8}$ cm^2/s (follicular phase), $D = (5.6 \pm 1.7) \cdot 10^{-8}$ cm^2/s (luteal phase), $D = (2.2 \pm 0.2) \cdot 10^{-8}$ cm^2/s (leiomyosarcoma), and $D = (1.1 \pm 0.4) \cdot 10^{-7}$ cm^2/s (serous carcinoma). The results obtained correspond to the literature data, taking into account the structural features of the tissues studied and the diffusion of highly concentrated glycerol in water as $D \approx 1.4 \cdot 10^{-7}$ cm^2/s [26]. Evidently, in tissue matrix rate of diffusion should be slow down as we see from the data presented.

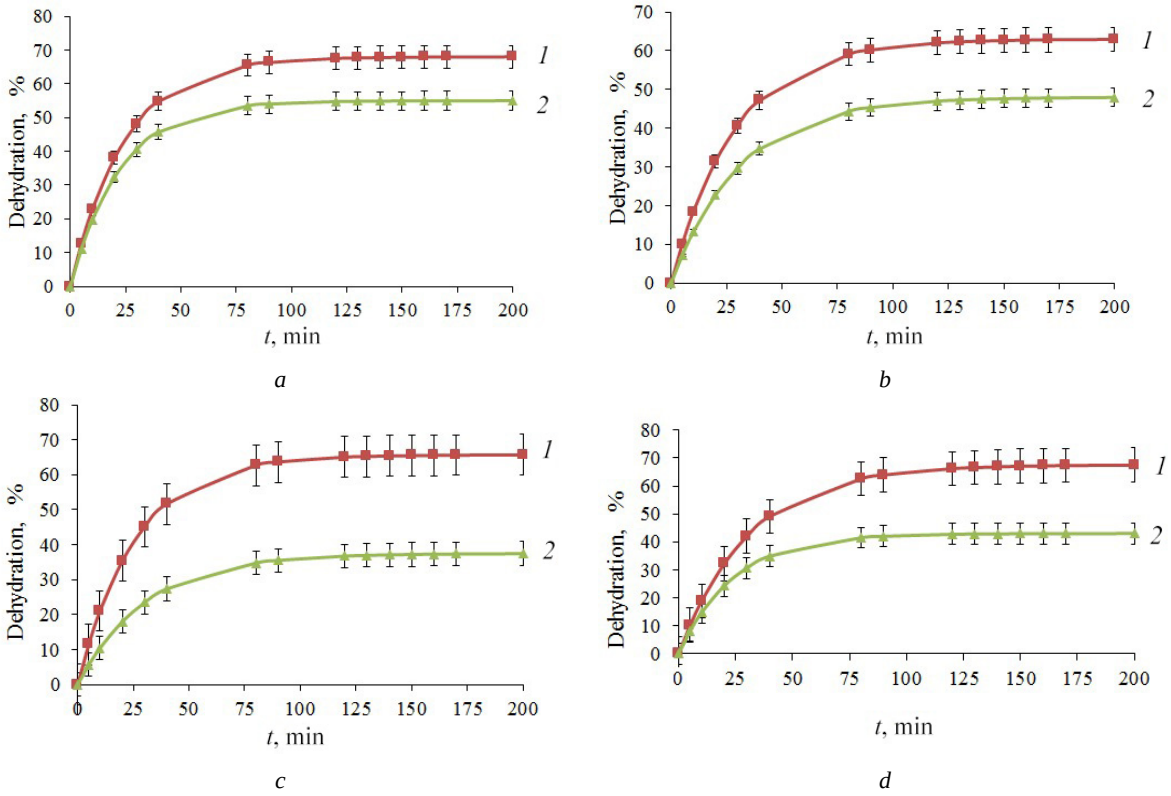

Figure 4. Kinetics of dehydration of cat ovarian samples: *1* – dehydration in air, *2* – dehydration when interacting with glycerol. Symbols represent experimental data, solid lines correspond to the least squares fit to equation (5), and bars are standard deviation values: healthy cat ovaries at the follicular phase (*a*) and at the luteal phase (*b*); cancerous ovaries with leimyosarcoma (*c*) and serous carcinoma (*d*) (color online)

Parameters of dehydration of cat ovarian tissue sections at their drying in air and at interaction with glycerol; for each type of samples, $n = 3$. See equations (4) and (5)

Sample type	Luteal phase	Follicular phase	Leiomyosarcoma	Serous carcinoma
In air				
$M(t=0)$, g	0.2065 ± 0.0013	0.2579 ± 0.0012	0.1819 ± 0.0015	0.2819 ± 0.0017
$M(t=$ 1.5 hrs), g	0.0613 ± 0.0011	0.0728 ± 0.0010	0.0967 ± 0.0016	0.0669 ± 0.0013
$M(t=$ 144 hrs), g (after complete evaporation of water)	0.0596 ± 0.001	0.0719 ± 0.0009	0.0946 ± 0.0012	0.0654 ± 0.0011
M_w, g (amount of movable (evaporated) water)	0.1469 ± 0.0009	0.1860 ± 0.0008	0.0873 ± 0.0004	0.2165 ± 0.0009
Percentage of water content in samples from the original mass, %	711	721	479	768
A_d (approximation)	0.63	0.68	0.657	0.676
In glycerol				
$M(t=0)$, g	0.1999 ± 0.0015	0.3264 ± 0.0017	0.2514 ± 0.0008	0.2678 ± 0.0009
$M(t=15$ hrs), g	0.1118 ± 0.0009	0.1620 ± 0.0012	0.1016 ± 0.0006	0.1558 ± 0.0009
M_w, g (amount of movable water at osmotic force, $t=1.5$ hrs)	0.0881 ± 0.0012	0.1644 ± 0.0014	0.1498 ± 0.0009	0.1120 ± 0.0010
M_w, g (interstitial water released into glycerol, obtained by measuring the refractive index of glycerol after 1.5 hrs of interaction)	0.0955 ± 0.0005	0.1009 ± 0.0010	0.1011 ± 0.0009	0.0985 ± 0.0008
Percentage of water content in samples from the original mass after 1.5 hrs of interaction with glycerol, %	47.8	30.9	40.2	36.8
M, g (glycerol, after 1.5 hrs of interaction)	0.0074 ± 0.0004	0.0635 ± 0.0006	0.0487 ± 0.0005	0.0135 ± 0.0005
A_d (approximation)	0.48	0.55	0.38	0.43
$M(t=48$ hrs), g	0.1069 ± 0.0006	0.1654 ± 0.0008	0.1007 ± 0.0007	0.1789 ± 0.0012
$M(t=72$ hrs), g	0.1908 ± 0.0004	0.1702 ± 0.0009	0.1046 ± 0.0014	0.1864 ± 0.0014
$M(t=96$ hrs), g	0.1218 ± 0.0007	0.1766 ± 0.0012	0.1098 ± 0.0009	0.2022 ± 0.0010
$M(t=216$ hrs), g	0.1412 ± 0.0005	0.2187 ± 0.0008	0.1206 ± 0.0011	0.2433 ± 0.0007
$M(t=408$ hrs), g	0.1781 ± 0.0010	0.2682 ± 0.0011	0.1283 ± 0.0008	0.2936 ± 0.0012

4. Conclusions

Four groups of cat ovarian samples were studied: healthy and with oncological pathology. Histological studies were performed to identify differences between these groups. Diffuse reflection spectra of ovary tissue sections in the follicular, luteal phases of the cycle, as well as ovary with leimyosarcoma and serous carcinoma were measured. The perfusion kinetics of healthy ovaries and ovaries with pathology under the influence of 99.5% glycerol were studied, on the base of which effective diffusion coefficient of tissue water was estimated for the ovaries of cats: $D = (2.6 \pm 0.4) \cdot 10^{-6}$ cm^2/s (follicular phase); $D = (3.3 \pm 0.4) \cdot 10^{-6}$ cm^2/s (luteal phase); $D = (3.0 \pm 0.3) \cdot 10^{-6}$ cm^2/s (leiomyosarcoma); $D = (1.6 \pm 0.2) \cdot 10^{-6}$ cm^2/s (serous carcinoma). Diffusion of glycerol occurs over a long period of time, about 400 hours, and for the samples under study diffusion coefficients were determined as the following: $D = (8.3 \pm 2.5) \cdot 10^{-8}$ cm^2/s (follicular phase), $D = (5.6 \pm 1.7) \cdot 10^{-8}$ cm^2/s (luteal phase), $D = (2.2 \pm 0.2) \cdot 10^{-8}$ cm^2/s (leiomyosarcoma), and $D = (1.1 \pm 0.4) \cdot 10^{-7}$ cm^2/s (serous carcinoma). It was revealed that the diffusion coefficients of tissue water under the influence of glycerol are different, which is directly related to the characteristics of the morphological structure of the organs under study. Using the obtained effective diffusion coefficient, it was possible to obtain the time of complete dehydration of the entire ovary under the influence of glycerol, which differs significantly for normal and pathological organs. Thus, it has been proven that when biological tissue interacts with glycerol, there is an outflow of interstitial water into the space occupied by glycerol (into the cuvette) and inflow of glycerol into the biological tissue. Successful cryopreservation and subsequent thawing of a transplanted ovary largely depend on knowledge of the quantitative characteristics of perfusion-kinetic processes during freezing and thawing of the organ, to ensure uniform distribution while minimizing exposure time

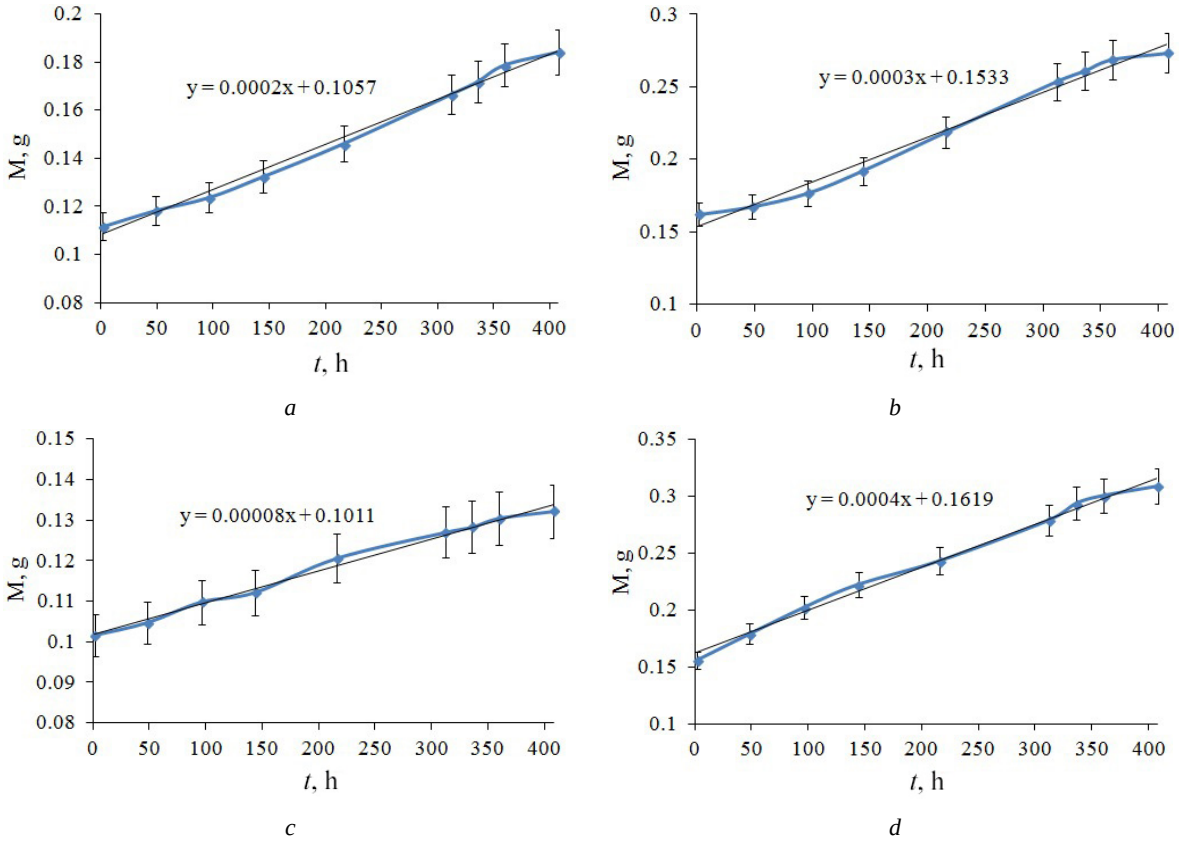

Figure 5. Kinetics of changes in the mass of the studied samples and approximation functions for determining the diffusion coefficient of glycerol in tissue: healthy cat ovaries at the follicular phase (*a*) and at the luteal phase (*b*); cancerous ovaries with leimyosarcoma (*c*) and serous carcinoma (*d*). The mass of samples at zero time ($t = 0$) was taken from Table 1 and showing value after 1.5 hours of interaction with glycerol, when tissue dehydration process was almost completed (color online)

and toxicity. Data obtained from this study can be used to design clinical protocols for drug delivery and organ cryopreservation, new reproductive technologies and ovarian implantation. It is of interest to obtain the diffusion-kinetic parameters of a number of other pharmaceuticals often used as cryopreservatives, for example, DMSO, ethylene glycol, etc. Knowledge of the optical properties of various biological tissues, in particular the ovaries, and their perfusion-kinetic characteristics is very important, it has both practical and theoretical significance in various scientific fields. There is a need to develop clinically accessible, accurate optical methods for monitoring normal and pathological metabolic cellular processes.

References

1. Sumanasekera W., Beckmann T., Fuller L., Castle M., Huff M. Epidemiology of Ovarian Cancer: Risk Factors and Prevention. *Biomed. J. Sci. & Tech. Res.*, 2018, vol. 11, no. 2, pp. 8405–8417. https://doi.org/10.26717/BJSTR.2018.11.002076
2. Laguerre M. D., Arkerson B. J., Robinson M. A., Moawad N. S. Outcomes of laparoscopic management of chronic pelvic pain and endometriosis. *J. Obstet. Gynecol.*, 2022, vol. 42, pp. 146–152. https://doi.org/10.1080/01443615.2021.1882967
3. Tuchin V. V. *Optical Clearing of Tissues and Blood*. Bellingham, WA, USA, SPIE Press, 2006. 408 p.
4. Tuchin V. V., Zhu D., Genina E. A. *Handbook of Tissue Optical Clearing: New Prospects in Optical Imaging*. Boca Raton, FL, USA, CRC Press, 2022. 410 p.
5. Tuchina D. K., Meerovich I. G., Sindeeva O. A., Zherdeva V. V., Savitsky A. P., Bogdanov A. A. Jr., Tuchin V. V. Magnetic resonance contrast agents in optical clearing: Prospects for multimodal tissue imaging. *J. Biophotonics*, 2020, vol. 13, article no. e201960249. https://doi.org/10.1002/jbio.201960249
6. Kazachkina N. I., Zherdeva V. V., Meerovich I. G., Saydasheva A. N., Solovyev I. D., Tuchina D. K., Savitsky A. P., Tuchin V. V., Bogdanov A. A. MR and fluorescence imaging of gadobutrol-induced optical clearing of red fluorescent protein signal in an *in vivo* cancer model. *NMR in Biomedicine*, 2022, vol. 35, no. 7, article no. e4708. https://doi.org/10.1002/nbm.4708
7. Silva H. F., Martins I. S., Bogdanov A. A. Jr., Tuchin V. V., Oliveira L. M. Characterization of optical clearing mechanisms in muscle during treatment with glycerol and gadobutrol solutions. *J. Biophotonics*, 2023,

vol. 16, no. 1, article no. e202200205. https://doi.org/10.1002/jbio.202200205

8. Wang T., Brewer M., Zhu Q. An overview of optical coherence tomography for ovarian tissue imaging and characterization. *Wiley Interdiscip. Rev. Nanomed. Nanobiotechnol.*, 2015, vol. 7, no. 1, pp. 1–16. https://doi.org/10.1002/wnan.1306
9. Hariri L. P., Bonnema G. T., Schmidt K., Winkler A. M., Korde V., Hatch K. D., Davis J. R., Brewer M. A., Barton J. K. Laparoscopic optical coherence tomography imaging of human ovarian cancer. *Gynecol. Oncol.*, 2009, vol. 114, no. 2, pp. 188–194. https://doi.org/10.1016/j.ygyno.2009.05.014
10. Sreyankar N., Melinda S., Quing Zh. Classification and analysis of human ovarian tissue using full field optical coherence tomography. *Biomedical Optics Express*, 2016, vol. 7, no. 1, article no. 5182. https://doi.org/10.1364/BOE.7.005182
11. Schwartz D., Sawyer T. W., Thurston N. Ovarian cancer detection using optical coherence tomography and convolutional neural networks. *Neural Comput & Applic.*, 2022, vol. 34, pp. 8977–8987. https://doi.org/10.1007/s00521-022-06920-3
12. Yang Y., Li X., Wang T., Kumavor P. D., Aguirre A., Shung K. K., Zhou Q., Sanders M., Brewer M., Zhu Q. Integrated optical coherence tomography, ultrasound and photoacoustic imaging for ovarian tissue characterization. *Biomed. Opt. Express*, 2011, vol. 9, no. 2, pp. 2551–2561. https://doi.org/10.1364/BO E.2.002551.
13. Del-Pozo-Lerida S., Salvador C., Martínez-Soler F., Tortosa A., Perucho M., Gimenez-Bonaf P. Preservation of fertility in patients with cancer (Review). *Oncol. Rep.*, 2019, vol. 41, pp. 2607–2614. https://doi.org/10.3892/or.2019.7063
14. Santos M. L., Pais A. S. Almeida Santos T. Fertility preservation in ovarian cancer patients. *Gynecol. Endocrinol.*, 2021, vol. 37, pp. 483–489.
15. Del Valle L., Corchon S., Palop J., Rubio J. M., Celda L. The experience of female oncological patients and fertility preservation: A phenomenology study. *Eur. J. Cancer Care*, 2022, vol. 31, article no. e13757. https://doi.org/10.1111/ecc.13757
16. Lee S., Ozkavukcu S., Ku S. Y. Current and Future Perspectives for Improving Ovarian Tissue Cryopreservation and Transplantation Outcomes for Cancer Patients. *Reprod. Sci.*, 2021, vol. 28, pp. 1746–1758. https://doi.org/10.1007/s43032-021-00517-2
17. Selifonov A. A., Rykhlov A. S., Tuchin V. V. *Ex vivo* study of the kinetics of ovarian tissue optical properties under the influence of 40%-glucose. *Izvestiya of Saratov University. Physics*, 2023, vol. 23, iss. 2, pp. 120–127. https://doi.org/10.18500/1817-3020-2023-23-2-120-127
18. Genina E. A., Bashkatov A. N., Korobko A. A., Zubkova E. A., Tuchin V. V., Yaroslavsky I. V., Altshuler G. B. Optical clearing of human skin: Comparative study of permeability and dehydration of intact and photothermally perforated skin. *J. Biomed. Opt.*, 2008, vol. 13, no. 2, pp. 021102–021108. https://doi.org/10.1117/1.2899149
19. Tuchina D. K., Bashkatov A. N., Genina E. A., Tuchin V. V. The effect of immersion agents on the weight and geometric parameters of myocardial tissue *in vitro*. *Biofizika*, 2018, vol. 63, no. 5, pp. 989–996. https://doi.org/10.1134/s0006350918050238
20. Selifonov A. A., Rykhlov A. S., Tuchin V. V. The Glycerol-Induced Perfusion-Kinetics of the Cat Ovaries in the Follicular and Luteal Phases of the Cycle. *Diagnostics*, 2023, vol. 13, no. 3, pp. 490. https://doi.org/10.3390/diagnostics13030490
21. Carneiro I., Carvalho S., Henrique R. A., Selifonov A., Oliveira L., Tuchin V. V. Enhanced Ultraviolet Spectroscopy by Optical Clearing for Biomedical Applications. *IEEE Journal of Selected Topics in Quantum Electronics*, 2021, vol. 27, pp. 1–8. https://doi.org/10.1109/jstqe.2020.3012350
22. Carneiro I., Carvalho S., Henrique R., Oliveira L., Tuchin V. V. A robust *ex vivo* method to evaluate the diffusion properties of agents in biological tissues. *J. Biophotonics*, 2019, vol. 12, e201800333. https://doi.org/10.1002/jbio.201800333
23. Oliveira L. R., Ferreira R. M., Pinheiro M. R., Silva H. F., Tuchin V. V., Oliveira L. M. Broadband spectral verification of optical clearing reversibility in lung tissue. *J. Biophotonics*, 2022, vol. 16, no. 1, e202200185. https://doi.org/10.1002/jbio.202200185
24. Han J., Sydykov B., Yang H., Sieme H., Oldenhof H., Wolkers W. F. Spectroscopic monitoring of transport processes during loading of ovarian tissue with cryoprotective solutions. *Sci. Rep.*, 2019, vol. 9. no. 1, pp. 15577. https://doi.org/10.1038/s41598-019-51903-5
25. Lotz J., Içli S., Liu D., Caliskan S., Sieme H., Wolkers W. F., Oldenhof H. Transport processes in equine oocytes and ovarian tissue during loading with cryoprotective solutions. *Biochim. Biophys. Acta. Gen. Subj.*, 2021, vol. 1865, article no. 129797. https://doi.org/10.1016/j.bbagen.2020.129797
26. D'Errico G., Ortona O., Capuano F., Vitagliano V. Diffusion Coefficients for the Binary System Glycerol + Water at 25 °C. A Velocity Correlation Study. *J. Chem. Eng.*, 2004, vol. 49, no. 6, pp. 1665–1670. https://doi.org/10.1021/je049917u

Поступила в редакцию 31.03.2024; одобрена после рецензирования 24.04.2024; принята к публикации 29.04.2024
The article was submitted 31.03.2024; approved after reviewing 24.04.2024; accepted for publication 29.04.2024